CERN Yellow Reports: Monographs CERN–2017–002-M
Volume 2/2017

Handbook of LHC Higgs cross sections:
4. Deciphering the nature of the Higgs sector

Report of the LHC Higgs Cross Section Working Group

Editors: D. de Florian
C. Grojean
F. Maltoni
C. Mariotti
A. Nikitenko
M. Pieri
P. Savard
M. Schumacher
R. Tanaka

CERN Yellow Reports: Monographs
Published by CERN, CH-1211 Geneva 23, Switzerland
ISBN 978–92–9083–442–7 (paperback)
ISBN 978–92–9083–443–4 (PDF)
Print ISSN 2519–8068
Online ISSN 2519–8076
DOI https://doi.org/10.23731/CYRM-2017-002
Accepted for publication by the CERN Report Editorial Board (CREB) on 6 April 2017
Available online at http://publishing.cern.ch/ and http://cds.cern.ch/

This volume is indexed in: CERN Document Server (CDS), INSPIRE.
This volume should be cited as:
LHC Higgs Cross Section Working Group, D. de Florian, C. Grojean, F. Maltoni, C. Mariotti, A. Nikitenko, M. Pieri, P. Savard, M. Schumacher, R. Tanaka (Eds.), Handbook of LHC Higgs Cross Sections: 4. Deciphering the nature of the Higgs sector, CERN Yellow Reports: Monographs, Vol. 2/2017, CERN-2017-002-M (CERN, Geneva, 2017), https://doi.org/10.23731/CYRM-2017-002

Abstract

This Report summarizes the results of the activities of the LHC Higgs Cross Section Working Group in the period 2014–2016. The main goal of the working group was to present the state-of-the-art of Higgs physics at the LHC, integrating all new results that have appeared in the last few years. The first part compiles the most up-to-date predictions of Higgs boson production cross sections and decay branching ratios, parton distribution functions, and off-shell Higgs boson production and interference effects. The second part discusses the recent progress in Higgs effective field theory predictions, followed by the third part on pseudo-observables, simplified template cross section and fiducial cross section measurements, which give the baseline framework for Higgs boson property measurements. The fourth part deals with the beyond the Standard Model predictions of various benchmark scenarios of Minimal Supersymmetric Standard Model, extended scalar sector, Next-to-Minimal Supersymmetric Standard Model and exotic Higgs boson decays. This report follows three previous working-group reports: *Handbook of LHC Higgs Cross Sections: 1. Inclusive Observables* (CERN-2011-002), *Handbook of LHC Higgs Cross Sections: 2. Differential Distributions* (CERN-2012-002), and *Handbook of LHC Higgs Cross Sections: 3. Higgs properties* (CERN-2013-004). The current report serves as the baseline reference for Higgs physics in LHC Run 2 and beyond.

We, the authors, would like to dedicate this Report to the memory of

Guido Altarelli (1941 - 2015)

Thomas Kibble (1932 - 2016)

and

Yoichiro Nambu (1921 - 2015)

Conveners

WG1: Higgs XS& BR: B. Mellado, P. Musella, M. Grazzini, R. Harlander

- *BR:* A. Denner, S. Heinemeyer, A. Mück, I. Puljak, D. Rebuzzi
- *ggF:* S. Forte, D. Gilberg, C. Hays, A. Lazopoulos, A. Massironi, G. Petrucciani, G. Zanderighi
- *VBF and WH/ZH:* S. Dittmaier, P. Govoni, B. Jäger, J. Nielsen, L. Perrozzi, E. Pianori, A. Rizzi, F. Tramontano
- *ttH/tH:* S. Guindon, C. Neu, S. Pozzorini, L. Reina

WG2: Higgs properties: M. Chen, M. Dührssen, A. David, A. Falkowski, C. Hays, G. Isidori

WG3: BSM Higgs: N. Rompotis, M. Pelliccioni, I. Low, M. Mühlleitner, R. Wolf

- *MSSM neutral:* R. Lane, S. Liebler, A. McCarn, P. Slavich, M. Spira, D. Winterbottom
- *MSSM charged:* M. Flechl, S. Sekula, M. Ubiali, M. Zaro
- *NMSSM:* U. Ellwanger, M. Mühlleitner, F. Staub, D. Strom, R. Yohay
- *Neutral extended scalars:* R. Gerosa, H. Logan, O. Stål, R. Santos, S. Su, X. Sun
- *Exotic decay:* S. Bressler, S. Gori, A. Mohammadi, J. Shelton

Cross-group task forces:

- *bbH/bH:* M. Beckingham, A. Nikitenko, M. Spira, M. Wiesemann
- *HH:* S. Dawson, C. Englert, M. Gouzevitch, R. Salerno, M. Slawinska
- *Fiducial cross-sections:* F.U. Bernlochner, S. Kraml, P. Milenovic, P. Monni
- *Offshell Higgs:* F. Caola, Y. Gao, N. Kauer, L. Soffi, J. Wang
- *MCnet:* S. Plätzer
- *PDF:* S. Forte, J. Huston, R. Thorne

Authors

D. de Florian[1], C. Grojean[2,3,4,5], F. Maltoni[6], C. Mariotti[7], A. Nikitenko[8], M. Pieri[9], P. Savard[10,11], M. Schumacher[12], R. Tanaka[13] (Eds.), R. Aggleton[14,15,16], M. Ahmad[17], B. Allanach[18], C. Anastasiou[19], W. Astill[20], S. Badger[21], M. Badziak[22,23,24], J. Baglio[25], E. Bagnaschi[2], A. Ballestrero[7], A. Banfi[26], D. Barducci[27], M. Beckingham[28], C. Becot[13,29], G. Bélanger[27], J. Bellm[30], N. Belyaev[31], F.U. Bernlochner[32], C. Beskidt[33], A. Biekötter[34], F. Bishara[20], W. Bizon[20], N.E. Bomark[35], M. Bonvini[20], S. Borowka[36], V. Bortolotto[37,38,39], S. Boselli[40], F.J. Botella[41], R. Boughezal[42], G.C. Branco[43], J. Brehmer[44], L. Brenner[45], S. Bressler[46], I. Brivio[47], A. Broggio[48], H. Brun[49], G. Buchalla[50], C.D. Burgard[12], A. Calandri[51], L. Caminada[36], R. Caminal Armadans[52], F. Campanario[53,54], J. Campbell[55], F. Caola[56,30], C.M. Carloni Calame[57], S. Carrazza[56], A. Carvalho[58], M. Casolino[5], O. Cata[50], A. Celis[50], F. Cerutti[24], N. Chanon[59], M. Chen[17], X. Chen[60], B. Chokoufé Nejad[2], N. Christensen[61], M. Ciuchini[62], R. Contino[63,56], T. Corbett[64], R. Costa[56,65], D. Curtin[66], M. Dall'Osso[58], A. David[56], S. Dawson[67], J. de Blas[68], W. de Boer[33], P. de Castro Manzano[58], C. Degrande[30], R.L. Delgado[69], F. Demartin[6], A. Denner[70], B. Di Micco[71], R. Di Nardo[56], S. Dittmaier[12], A. Dobado[69], T. Dorigo[58], F.A. Dreyer[72,73,56], M. Dührssen[56], C. Duhr[56,6], F. Dulat[74], K. Ecker[75], K. Ellis[30], U. Ellwanger[76], C. Englert[77], D. Espriu[78], A. Falkowski[76], L. Fayard[13], R. Feger[70], G. Ferrera[79], A. Ferroglia[80,81], N. Fidanza[82,1], T. Figy[83], M. Flechl[84], D. Fontes[43], S. Forte[85], P. Francavilla[86,87], E. Franco[68], R. Frederix[48], A. Freitas[88], F.F. Freitas[26], F. Frensch[33], S. Frixione[89], B. Fuks[72,73], E. Furlan[19], S. Gadatsch[56], J. Gao[42], Y. Gao[90], M.V. Garzelli[91], T. Gehrmann[36], R. Gerosa[9], M. Ghezzi[92], D. Ghosh[46], S. Gieseke[54], D. Gillberg[93], G.F. Giudice[56], E.W.N. Glover[30], F. Goertz[56], D. Gonçalves[30], J. Gonzalez-Fraile[44], M. Gorbahn[94], S. Gori[95], C.A. Gottardo[58], M. Gouzevitch[96], P. Govoni[97], D. Gray[29,98], M. Grazzini[36], N. Greiner[36], A. Greljo[36,99], J. Grigo[100], A.V. Gritsan[101], R. Gröber[62,30], S. Guindon[102], H.E. Haber[103], C. Han[104], T. Han[88], R. Harlander[34], M.A. Harrendorf[33], H.B. Hartanto[34], C. Hays[105], S. Heinemeyer[106,107,108], G. Heinrich[75], M. Herrero[47], F. Herzog[45], B. Hespel[6], V. Hirschi[74], S. Hoeche[74], S. Honeywell[109], S.J. Huber[26], C. Hugonie[110], J. Huston[111], A. Ilnicka[36,112], G. Isidori[36], B. Jäger[25], M. Jaquier[12], S.P. Jones[75], A. Juste[4,5], S. Kallweit[113], A. Kaluza[114], A. Kardos[115], A. Karlberg[20], Z. Kassabov[116,85], N. Kauer[117], D.I. Kazakov[118,33], M. Kerner[75], W. Kilian[119], F. Kling[120,55], K. Köneke[12], R. Kogler[121], R. Konoplich[29,98], S. Kortner[75], S. Kraml[122], C. Krause[50], F. Krauss[30], M. Krawczyk[22], A. Kulesza[123], S. Kuttimalai[30], R. Lane[124], A. Lazopoulos[19], G. Lee[125], P. Lenzi[126], I.M. Lewis[127], Y. Li[55], S. Liebler[2], J. Lindert[36], X. Liu[66], Z. Liu[55], F.J. Llanes-Estrada[69], H.E. Logan[93], D. Lopez-Val[6], I. Low[42,128], G. Luisoni[56], P. Maierhöfer [12], E. Maina[116], B. Mansoulié[129], H. Mantler[53,54], M. Mantoani[130], A.C. Marini[131], V.I. Martinez Outschoorn[52], S. Marzani[132], D. Marzocca[36], A. Massironi[133], K. Mawatari[122], J. Mazzitelli[82,134], A. McCarn[135], B. Mellado[136], K. Melnikov[100], S.B. Menari[137], L. Merlo[47], C. Meyer[138], P. Milenovic[56], K. Mimasu[26], S. Mishima[139], B. Mistlberger[56], S.-O. Moch[91], A. Mohammadi[140], P.F. Monni[20], G. Montagna[40], M. Moreno Llácer[130], N. Moretti[36], S. Moretti[15], L. Motyka[141], A. Mück[34], M. Mühlleitner[54], S. Munir[142], P. Musella[112], P. Nadolsky[143], D. Napoletano[30], M. Nebot[41], C. Neu[144], M. Neubert[113], R. Nevzorov[145,146], O. Nicrosini[57], J. Nielsen[103], K. Nikolopoulos[147], J.M. No[26], C. O'Brien[117], T. Ohl[70], C. Oleari[97], T. Orimoto[133], D. Pagani[6], C.E. Pandini[86], A. Papaefstathiou[56], A.S. Papanastasiou[148], G. Passarino[116], B.D. Pecjak[30], M. Pelliccioni[7], G. Perez[54], L. Perrozzi[112], F. Petriello[149,42], G. Petrucciani[56], E. Pianori[28], F. Piccinini[57], M. Pierini[56], A. Pilkington[137], S. Plätzer[30,137], T. Plehn[44], R. Podskubka[54], C.T. Potter[150], S. Pozzorini[36], K. Prokofiev[39,151], A. Pukhov[152], I. Puljak[153], M. Queitsch-Maitland[137], J. Quevillon[154], D. Rathlev[2], M. Rauch[54], E. Re[27], M.N. Rebelo[43], D. Rebuzzi[40], L. Reina[109], C. Reuschle[109], J. Reuter[2], M. Riembau[5,2], F. Riva[56], A. Rizzi[155], T. Robens[156], R. Röntsch[100], J. Rojo[20], J.C. Romão[43], N. Rompotis[157], J. Roskes[101], R. Roth[54], G.P. Salam[56], R. Salerno[158], M.O.P. Sampaio[65], R. Santos[159,160], V. Sanz[26], J.J. Sanz-Cillero[47], H. Sargsyan[36], U. Sarica[101], P. Schichtel[30], J. Schlenk[75], T. Schmidt[12], C. Schmitt[114], M. Schönherr[36], U. Schubert[75], M. Schulze[56], S. Sekula[143], M. Sekulla[54],

E. Shabalina[130], H.S. Shao[56], J. Shelton[52], C.H. Shepherd-Themistocleous[16], S.Y. Shim[2], F. Siegert[156], A. Signer[161,36], J.P. Silva[43], L. Silvestrini[68], M. Sjodahl[162], P. Slavich[163,73], M. Slawinska[45], L. Soffi[164], M. Spannowsky[30], C. Speckner[12], D.M. Sperka[165], M. Spira[92], O. Stål[166], F. Staub[56], T. Stebel[141], T. Stefaniak[103], M. Steinhauser[100], I.W. Stewart[131], M.J. Strassler[167], J. Streicher[54], D.M. Strom[150], S. Su[120], X. Sun[17], F.J. Tackmann[2], K. Tackmann[2], A.M. Teixeira[168], R. Teixeira de Lima[133], V. Theeuwes[132], R. Thorne[169], D. Tommasini[170], P. Torrielli[116], M. Tosi[56], F. Tramontano[171], Z. Trócsányi[115], M. Trott[172], I. Tsinikos[6], M. Ubiali[148], P. Vanlaer[49], W. Verkerke[45], A. Vicini[85], L. Viliani[126], E. Vryonidou[6], D. Wackeroth[132], C.E.M. Wagner[173,42], J. Wang[165], S. Wayand[33], G. Weiglein[2], C. Weiss[2,119], M. Wiesemann[36], C. Williams[132], J. Winter[111], D. Winterbottom[8], R. Wolf[33], M. Xiao[101], L.L. Yang[174,175,60], R. Yohay[109], S.P.Y. Yuen[176], G. Zanderighi[56,20], M. Zaro[72,73], D. Zeppenfeld[54], R. Ziegler[73], T. Zirke[75], and J. Zupan[95]

1 International Center for Advanced Studies, UNSAM, 1650 Buenos Aires, Argentina
2 DESY, 22607 Hamburg, Germany
3 Institut für Physik, Humboldt-Universität zu Berlin, 12489 Berlin, Germany
4 Institució Catalana de Recerca i Estudis Avançats, 08010 Barcelona, Spain
5 Institut de Física d'Altes Energies, Barcelona Institute of Science and Technology (BIST), 08193 Bellaterra, Barcelona, Spain
6 Centre for Cosmology, Particle Physics and Phenomenology (CP3), Université catholique de Louvain, 1348 Louvain-la-Neuve, Belgium
7 INFN Sezione di Torino, 10125 Torino, Italy
8 High Energy Physics Group, Blackett Lab., Imperial College, SW7 2AZ London, UK
9 University of California San Diego, CA 92093, USA
10 University of Toronto, Toronto, ON M5S 1A7, Canada
11 TRIUMF, Vancouver, BC V6T 2A3, Canada
12 Physikalisches Institut, Albert-Ludwigs-Universität Freiburg, 79104 Freiburg, Germany
13 LAL, Université de Paris-Sud, 91405 Orsay, France
14 University of Bristol, Bristol BS8 1TL, UK
15 School of Physics and Astronomy, University of Southampton, Highfield SO17 1BJ, UK
16 Rutherford Appleton Laboratory, Didcot OX110QX, UK
17 Institute of High Energy Physics, Beijing 100049, China
18 DAMTP, CMS, University of Cambridge, CB3 0WA Cambridge, UK
19 Institute for Theoretical Physics, Physics Department, ETH Zürich, 8093 Zurich, Switzerland
20 Rudolf Peierls Centre for Theoretical Physics, University of Oxford, OX1 3NP Oxford, UK
21 Higgs Centre for Theoretical Physics, School of Physics and Astronomy, University of Edinburgh, EH9 3JZ Edinburgh, Scotland, UK
22 Institute of Theoretical Physics, Faculty of Physics, University of Warsaw, 02-093 Warsaw, Poland
23 Berkeley Center for Theoretical Physics, Department of Physics, University of California, Berkeley, CA 94720, USA
24 Lawrence Berkeley National Laboratory, Berkeley, CA 94720, USA
25 Institute for Theoretical Physics, University of Tübingen, 72076 Tübingen, Germany
26 Department of Physics and Astronomy, University of Sussex, BN1 9QH Brighton, UK
27 LAPTh, Université Savoie Mont Blanc, CNRS, 74941 Annecy-le-Vieux, France
28 Department of Physics, University of Warwick, CV4 7AL Warwick, UK
29 Department of Physics, New York University, New York, NY 10003, USA
30 Institute for Particle Physics Phenomenology, Department of Physics, Durham University, Durham DH1 3LE, UK
31 National Research Nuclear University MEPhI (Moscow Engineering Physics Institute), 115409 Moscow, Russia
32 Physikalisches Institut der Rheinische Friedrich-Wilhelms-Universität Bonn, 53115 Bonn, Ger-

many
[33] Institut für Experimentelle Kernphysik, Karlsruhe Institute of Technology, 76128 Karlsruhe, Germany
[34] Institut für Theoretische Teilchenphysik und Kosmologie, RWTH Aachen University, 52056 Aachen, Germany
[35] University of Agder, 4604 Kristiansand, Norway
[36] Physik-Institut, Universität Zürich, 8057 Zurich, Switzerland
[37] Department of Physics, The Chinese University of Hong Kong, Shatin, Hong Kong
[38] Department of Physics, The University of Hong Kong, Hong Kong
[39] Department of Physics, The Hong Kong University of Science and Technology, Hong Kong
[40] Dipartimento di Fisica, Università di Pavia, and INFN, Sezione di Pavia, 27100 Pavia, Italy
[41] Departamento de Física Teórica and IFIC, Universitat de València-CSIC, 46100 Burjassot, Spain
[42] High Energy Physics Division, Argonne National Laboratory, Argonne, IL 60439, USA
[43] Departamento de Física and CFTP, Instituto Superior Técnico, Universidade de Lisboa, 1049-001 Lisboa, Portugal
[44] Institut für Theoretische Physik, Universität Heidelberg, 69120 Heidelberg, Germany
[45] Nikhef, Science Park 105, 1098 XG Amsterdam, The Netherlands
[46] Department of Particle Physics and Astrophysics, Weizmann Institute of Science, 7610001 Rehovot, Israel
[47] Departamento de Física Teórica and Instituto de Física Teórica, IFT-UAM/CSIC, Universidad Autónoma de Madrid, Cantoblanco, 28049 Madrid, Spain
[48] Technische Universität München, 85748 Garching, Germany
[49] Université Libre de Bruxelles, Service de physique des particules élémentaires, 1050 Bruxelles, Belgium
[50] Ludwig-Maximilians-Universität München, Fakultät für Physik, Arnold Sommerfeld Center for Theoretical Physics, 80333 München, Germany
[51] CPPM, Université Aix-Marseille, 13288 Marseille, France
[52] Department of Physics, University of Illinois at Urbana-Champaign, Urbana, IL 61801, USA
[53] Institute for Nuclear Physics, Karlsruhe Institute of Technology, 76344 Eggenstein-Leopoldshafen, Germany
[54] Institute for Theoretical Physics, Karlsruhe Institute of Technology, 76128 Karlsruhe, Germany
[55] Theoretical Physics Department, Fermilab, Batavia, IL 60510, USA
[56] CERN, 1211 Geneva 23, Switzerland
[57] INFN, Sezione di Pavia, 27100 Pavia, Italy
[58] Dipartimento di Fisica e Astronomia, Università di Padova and INFN, Sezione di Padova, 35131 Padova, Italy
[59] IPHC, Université de Strasbourg, CNRS/IN2P3, 67037 Strasbourg, France
[60] Center for High Energy Physics, Peking University, Beijing 100871, China
[61] Illinois State University, Normal, IL 61790, USA
[62] INFN, Sezione di Roma Tre, 00146 Roma, Italy
[63] Institut de Théorie des Phénomènes Physiques, EPFL, 1015 Lausanne, Switzerland
[64] ARC CoEPP, University of Melbourne, Victoria 3010, Australia
[65] Departamento de Física da Universidade de Aveiro and CIDMA, 3810-183 Aveiro, Portugal
[66] Maryland Center for Fundamental Physics, Department of Physics, University of Maryland, MD 20742, USA
[67] Brookhaven National Laboratory, Upton, NY 11973, USA
[68] INFN, Sezione di Roma, 00185 Roma, Italy
[69] Departamento de Física Teórica I, Universidad Complutense, 28040-Madrid. Spain
[70] Institut für Theoretische Physik und Astrophysik, 97074 Würzburg, Germany
[71] Università degli Studi di Roma Tre and INFN,Sezione di Roma Tre, 00146 Roma, Italy

[72] Sorbonne Universités, Université Pierre et Marie Curie Paris 06, LPTHE, 75005 Paris, France
[73] CNRS, UMR 7589, LPTHE, 75005, Paris France
[74] SLAC National Accelerator Laboratory, Menlo Park, CA 94025, USA
[75] Max-Planck-Institut für Physik, 80805 München, Germany
[76] LPT, UMR 8627, CNRS, Université de Paris-Sud, Université Paris-Saclay, 91405 Orsay, France
[77] SUPA, School of Physics and Astronomy, University of Glasgow, G12 8QQ Glasgow, UK
[78] Institute of Cosmos Sciences, Universitat de Barcelona, 08028 Barcelona, Spain
[79] Dipartimento di Fisica, Universit'a di Milano and INFN, Sezione di Milano, 20133 Milan, Italy
[80] New York City College of Technology, Brooklyn, NY 11201, USA
[81] The Graduate School and University Center, The City University of New York, New York, NY 10016 USA
[82] Departamento de Física, FCEyN, Universidad de Buenos Aires, Capital Federal, Argentina
[83] Department of Mathematics, Statistics, and Physics, Wichita State University, Wichita, KS 67206, USA
[84] Institute of High Energy Physics, Austrian Academy of Sciences, 1050 Wien, Austria
[85] Tif Lab, Dipartimento di Fisica, Università di Milano, and INFN, Sezione di Milano, 20133 Milano, Italy
[86] LPNHE, Université Pierre et Marie Curie and Université Paris-Diderot, 75005 Paris, France
[87] Institut Lagrange de Paris, Université Pierre et Marie Curie, 75005 Paris, France
[88] Department of Physics and Astronomy, University of Pittsburgh, Pittsburgh, PA 15260, USA
[89] INFN, Sezione di Genova, 16146 Genova, Italy
[90] Department of Physics, University of Liverpool, L69 7ZE Liverpool, UK
[91] II. Institut für Theoretische Physik, Universität Hamburg, 22761 Hamburg, Germany
[92] Paul Scherrer Institut, 5323 Villigen PSI, Switzerland
[93] Physics Department, Carleton University, Ottawa, ON K1S 5B6 Canada
[94] Department of Mathematical Sciences, University of Liverpool, L69 7ZL Liverpool, UK
[95] Department of Physics, University of Cincinnati, Cincinnati, OH 45221, USA
[96] Université de Lyon, Université Claude Bernard Lyon 1, CNRS-IN2P3, IPNL, 69622 Villeurbanne, France
[97] Università Milano-Bicocca and INFN, Sezione di Milano-Bicocca, 20126 Milano, Italy
[98] Physics Department, Manhattan College, Riverdale, New York, NY 10471, USA
[99] Faculty of Science, University of Sarajevo, 71000 Sarajevo, Bosnia and Herzegovina
[100] Institute for Theoretical Particle Physics, Karlsruhe Institute of Technology, 76128 Karlsruhe, Germany
[101] Department of Physics and Astronomy, Johns Hopkins University, Baltimore, MD 21218, USA
[102] Physics Department, SUNY Albany, Albany, NY 12222, USA
[103] Santa Cruz Institute for Particle Physics (SCIPP) and Department of Physics, University of California, Santa Cruz, CA 95064, USA
[104] Kavli IPMU (WPI), UTIAS, University of Tokyo, Kashiwa, 277-8583, Japan
[105] Department of Physics, Oxford University, OX1 3RH Oxford, UK
[106] Instituto de Física Teórica, IFT-UAM/CSIC, Universidad Autónoma de Madrid, Cantoblanco, 28049 Madrid, Spain
[107] Campus of International Excellence UAM+CSIC, Cantoblanco, 28049 Madrid, Spain
[108] Instituto de Física de Cantabria (CSIC/UC), 39005 Santander, Spain
[109] Physics Department, Florida State University, Tallahassee, FL 32306, USA
[110] LUPM, UMR 5299, CNRS, Université de Montpellier, 34095 Montpellier, France
[111] Department of Physics and Astronomy, Michigan State University, East Lansing, MI 48824, USA
[112] Institute for Particle Physics, Physics Department, ETH Zürich, 8093 Zurich, Switzerland
[113] PRISMA Cluster of Excellence, Johannes Gutenberg University, 55099 Mainz, Germany
[114] Institut für Physik, Johannes Gutenberg-Universität, 55099 Mainz, Germany

[115] University of Debrecen and MTA-DE Particle Physics Research Group, 4002 Debrecen, Hungary
[116] Dipartimento di Fisica, Università di Torino, INFN Sezione di Torino, 10125 Torino, Italy
[117] Department of Physics, Royal Holloway, University of London, Egham Hill, Egham TW20 0EX, UK
[118] Bogoliubov Laboratory of Theoretical Physics, Joint Institute for Nuclear Research, 141980 Dubna, Moscow Region, Russia
[119] Department of Physics, University of Siegen, 57068 Siegen, Germany
[120] Department of Physics, University of Arizona, Tucson, AZ 85721, USA
[121] Institut für Experimentalphysik, Universität Hamburg, 22761 Hamburg, Germany
[122] LPSC, Université Grenoble-Alpes, CNRS/IN2P3, 38026 Grenoble, France
[123] Institute for Theoretical Physics, WWU Münster, 48149 Münster, Germany
[124] High Energy Physics Group, Blackett Laboratory, Imperial College, SW7 2AZ London, UK
[125] Physics Department, Technion, Haifa 32000, Israel
[126] Università and INFN, Sezione di Firenze, 50019 Firenze, Italy
[127] Department of Physics and Astronomy, University of Kansas, Lawrence, KS 66045, USA
[128] Department of Physics and Astronomy, Northwestern University, Evanston, IL 60208, USA
[129] CEA IRFU-SPP, 91191 Gif-sur-Yvette, France
[130] II.Physikalisches Institut Universität Goettingen 37077 Germany
[131] CTP, MIT, Cambridge, MA 02139, USA
[132] Department of Physics, University at Buffalo, The State University of New York, Buffalo, NY 14260, USA
[133] Department of Physics, Northeastern University, Boston, MA 02115, USA
[134] International Center for Advanced Studies, UNSAM, 1650 Buenos Aires, Argentina
[135] Department of Physics, The University of Michigan, Ann Arbor, MI 48104, USA
[136] University of the Witwatersrand, School of Physics, Private Bag 3, Wits 2050, South Africa
[137] School of Physics and Astronomy, University of Manchester, Manchester, M13 9PL, UK
[138] Department of Physics, University of Pennsylvania, Philadelphia, PA 19104, USA
[139] Theory Center, Institute of Particle and Nuclear Studies, KEK, Tsukuba, 305-0801, Japan
[140] Kansas State University, Manhattan, KS, 66506, USA
[141] M. Smoluchowski Institute of Physics, Jagiellonian University, Krakow, 30-348 Poland
[142] KIAS, Seoul 130-722, Republic of Korea
[143] Department of Physics, Southern Methodist University, Dallas, TX 75275, USA
[144] University of Virginia, Charlottesville, VA 22903, USA
[145] ARC Centre of Excellence for Particle Physics at the Terascale and CSSM, Department of Physics, The University of Adelaide, Adelaide SA 5005, Australia
[146] Institute for Theoretical and Experimental Physics, Moscow 117218, Russia
[147] University of Birmingham, Birmingham B15 2TT, UK
[148] University of Cambridge, The Cavendish Laboratory, CB3 0HE Cambridge, UK
[149] Department of Physics and Astronomy, Northwestern University, Evanston, IL 60208, USA
[150] Center for High Energy Physics, University of Oregon, Eugene, OR 97403, USA
[151] HKUST Jockey Club Institute for Advanced Study, Hong-Kong
[152] Lomonosov Moscow State University, Skobeltsyn Institute of Nuclear, Moscow 119992, Russia
[153] University of Split, 21000 Split, Croatia
[154] King's College London, WC2R 2LS London, UK
[155] Dipartimento di Fisica Università di Pisa, and INFN, Sezione di Pisa, 56100 Pisa, Italy
[156] Institut für Kern- und Teilchenphysik, TU Dresden, 01069 Dresden, Germany
[157] University of Washington, Physics Department, Seattle WA 98195, USA
[158] LLR, IN2P3-CNRS, École Polytechnique, 91128 Palaiseau, France
[159] ISEL - Instituto Superior de Engenharia de Lisboa, Instituto Politécnico de Lisboa, 1959-007 Lisboa, Portugal

[160] Centro de Física Teórica e Computacional, Faculdade de Ciências, Universidade de Lisboa, 1749-016 Lisboa, Portugal
[161] Paul Scherrer Institut, 5232 Villigen PSI, Switzerland
[162] Department of Astronomy and Theoretical Physics, Lund University, 22362 Lund, Sweden
[163] Sorbonne Universités, UPMC Univ. Paris 06, LPTHE, 75005 Paris, France
[164] Cornell University, Ithaca, NY 14850, USA
[165] University of Florida, Gainesville, FL 32611, USA
[166] The Oskar Klein Centre, Department of Physics, Stockholm University, 106 91 Stockholm, Sweden
[167] Department of Physics, Harvard University, Cambridge, MA 02138, USA
[168] LPC, CNRS/IN2P3 UMR 6533, 63171 Aubière, France
[169] University College London, WC 1E 6BT London, UK
[170] Institute of Nuclear and Particle Physics, NCSR Demokritos, 15310 Agia Paraskevi, Greece
[171] Dipartimento di Fisica "E. Pancini", Università di Napoli Federico II and INFN, Sezione di Napoli, 80126 Napoli, Italy
[172] Niels Bohr International Academy, University of Copenhagen, Blegdamsvej 17, 2100 Copenhagen, Denmark
[173] Enrico Fermi Institute, Kavli Institute for Cosmological Physics, University of Chicago, Chicago, IL 60637, USA
[174] School of Physics and State Key Laboratory of Nuclear Physics and Technology, Peking University, Beijing 100871, China
[175] Collaborative Innovation Center of Quantum Matter, Beijing 100084, China
[176] Physikalisches Institut der Universität Bonn, 53115 Bonn, Germany

Contents

Chapter I.2

Parton Distribution Functions

S. Forte, J. Huston, R. S. Thorne (Eds.); S. Carrazza, J. Gao, Z. Kassabov, P. Nadolsky, J. Rojo

I.2.1 The PDF4LHC recommendation

Previous Yellow Reports [7–9] have provided snapshots of the state-of-the-art for PDF determination, along with recommendations for PDF use, and for calculations of PDF uncertainties, following the guidance of the PDF4LHC group. In a previous recommendation [28], three PDF sets were used: CT10 [29], MSTW2008 [30] and NNPDF2.3 [31]. These were global PDF fits involving data from a variety of experiments, including collider data from the Tevatron. The uncertainty was provided by the envelope of all three PDF error sets, and the central prediction as mid-point of this envelope. This choice is conservative but not ideal, in that it tends to be dominated by error PDFs at the edge of the uncertainty band; it was adopted because it was felt that the degree of agreement of the PDF sets was not sufficient to warrant their statistical combination. Specifically, agreement was unsatisfactory for the gluon distribution, particularly in the region appropriate for Higgs boson production through gluon-gluon fusion. This disagreement prompted an intensive year-long study by the three global PDF groups, along with HERAPDF [32], but this did not uncover a clear explanation for the differences [33].

Prior to the writing of YR4, the major PDF groups have released updates to their PDF fits, at NLO and NNLO, including in most cases data from the LHC [34]. The new PDF4LHC recommendation [35] uses the updated PDFs from the three global PDF groups included in the previous recommendation: CT14 [36], MMHT14 [37] and NNPDF3.0 [38], respectively. Details as to why this choice was made can be found in the PDF4LHC document. The primary requirements are that the PDFs should be based on global datasets, be carried out in a general-mass variable flavour-number scheme, and have compatible values for the QCD coupling constant $\alpha_s(m_Z)$. As we shall see shortly, these new PDF sets are in good agreement, not only in the quark sector (where the agreement was satisfactory already in the previous generation of PDFs) but also for the gluon. The changes can be ascribed partially to the addition of new data sets used in the PDF fits, but primarily to improvements in the fitting formalisms. This level of agreement may change in detail with future updates, but generally the good level of agreement should stay. An alternative recommendation [39] is that all PDFs (ABM12 [40], CJ15 [41], CT14 [36], HERAPDF2.0 [32], JR14 [42], HERAPDF2.0 [32] MMHT14 [37], NNPDF3.0 [38]) and accompanying coupling and quark mass variation should be used for precision theory predictions and any `LHAPDF6` [43] PDF set for other predictions.

Currently, there are two different representations of PDF uncertainties: the Monte Carlo representation [44, 45] and the Hessian representation [46]. Both provide compatible descriptions of the PDF uncertainties, and recent developments have allowed for the straight-forward conversion of one representation to the other [47–49]. The use of the Monte Carlo representation makes possible a statistical combination of different PDF sets. If different PDF sets can be assured to be equally likely representations of the underlying PDF probability distribution, they can be combined simply by taking their un-weighted average. This can be arrived at by generating equal numbers of Monte Carlo replicas from each input PDF set, and then merging the replica sets. The NNPDF3.0 PDF set is naturally in this format. For the Hessian sets, CT14 and MMHT2014, the Monte Carlo replicas are generated by sampling along the eigenvector directions, assuming a Gaussian distribution.

Combinations in this manner are most appropriate when the PDF sets that are combined are compatible with each other, as CT14, MMHT2014 and NNPDF3.0 are. Such a combination also allows for a direct statistical interpretation of the resulting PDF uncertainties, unlike the envelope method. Monte

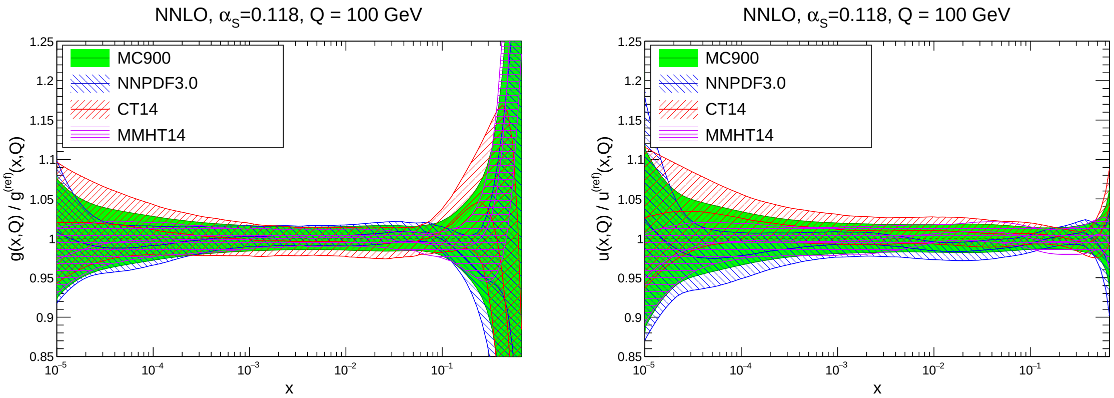

Figure 2: Comparison of the MC900 PDFs with the sets that enter the combination: CT14, MMHT14 and NNPDF3.0 at NNLO. We show the gluon and the up quark at $Q = 100$ GeV. Results are normalized to the central value of the prior set MC900.

Carlo combinations of these three PDFs have been provided at both NLO and NNLO by the PDF4LHC working group. In the following discussion we concentrate on NNLO; similar considerations apply to NLO.

It was determined that $N_{\rm rep} = 900$ Monte Carlo replicas, combining $N_{\rm rep} = 300$ replicas from each of the three individual PDF sets, were sufficient to represent the combined PDF probability distribution. In Figure 2 we show a comparison of the combined PDF4LHC15 NNLO set (indicated by MC900 in the plot) with the three sets that enter the combination, CT14, MMHT14 and NNPDF3.0. We show the gluon and the up quark at $Q = 100$ GeV, normalized to the central value of the PDF4LHC15 combination. In these plots, as in the rest of this chapter, we use a fixed value $\alpha_s(m_Z) = 0.118$.

It can be seen that in the "precision physics" region, roughly from $x \simeq 0.001$ to $x \simeq 0.1$, the PDFs from the three global sets agree reasonably well with each other, with perfect agreement for the gluon, and less good agreement for the up quark. This is reflected in the combined PDF4LHC15 set, constructed from the three input PDF sets. On the other hand, at low and high values of x, the uncertainty bands from the three PDF sets differ, and the uncertainty band for the 900 Monte Carlo replicas is smaller than the envelope of the three PDF uncertainty bands. These are regions in which PDFs are only weakly constrained by data, as seen by the increasingly large size of the uncertainty, and the inflated uncertainty in the combination appears to provides a reasonable estimate.

In Figure 3 we compare the NNLO PDF luminosities at the LHC 13 TeV computed using the prior set PDF4LHC15 NNLO, both to the three sets which were used for the previous PDF4LHC recommendation (CT10, MSTW08 and NNPDF2.3), and the three sets which enter the current combination CT14, MMHT14 and NNPDF3.0 NNLO. We show the gg and $q\bar{q}$ luminosities as a function of the invariant mass of the final state M_X, normalized to the central value of `PDF4LHC15_nnlo_prior`. The improvement in compatibility of the new sets in comparison to the old ones, especially in the gluon sector, is apparent, particularly in the precision mass region, say roughly 50 GeV to 1 TeV (more so for gg than for $q\bar{q}$). Reassuringly, even though uncertainty estimates differ somewhat between current sets, especially for quarks, central values of all sets in this region are in good agreement. Interestingly, they also agree well with the mid-point of the envelope of the old sets. Hence, in practice, in the precision region, the central prediction with the old prescription (the envelope of CT10, MSTW08, and NNPDF2.3) and the new prescription (the PDF4LHC15 combined set) are actually quite close.

There is more disagreement in the low mass region and in the high mass region, and the range of uncertainty for the 900 set Monte Carlo can be less than the envelope of the three PDF groups. This is not surprising, as the combined uncertainty band reflects the common trend of all input PDF ensembles, while the envelope unduly emphasizes extreme behaviour of a few replicas. While the combined

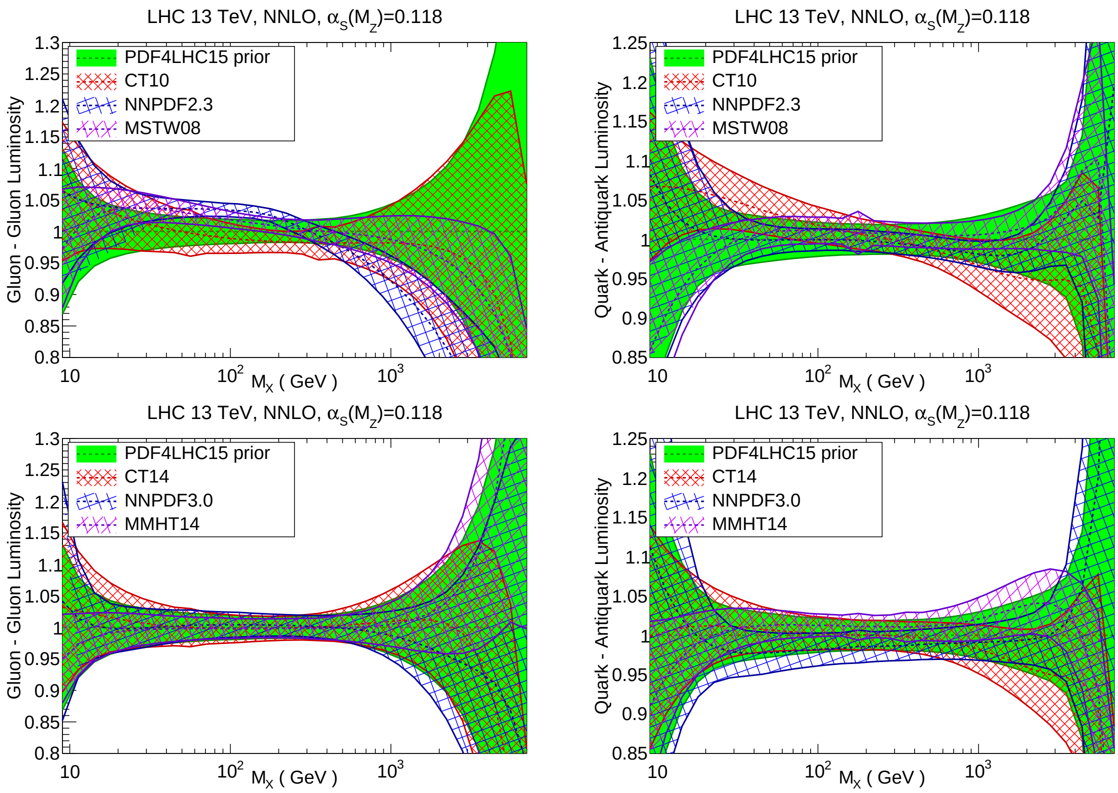

Figure 3: Comparison of NNLO parton luminosities at the LHC 13 TeV. Top: the PDF4LHC15 combined set compared to the CT10, MSTW08, and NNPDF2.3 PDF set whose envelope was used as a previous PDF4LHC recommendation. Bottom: the PDF4LHC15 combined set compared to the three individual sets which enter the combination: CT14, MMHT14 and NNPDF3.0. The gg (left) and the $q\bar{q}$ (right) luminosities are shown as a function of the invariant mass of the final state M_X, normalized to the central value of `PDF4LHC15_nnlo_prior`.

uncertainty appears to be conservative enough, this should be kept in mind especially in discussions of uncertainties of high-mass searches.

I.2.2 The PDF4LHC15 PDF sets

Although the $N_{\rm rep} = 900$ Monte Carlo set itself could be used to determine PDF uncertainties for any LHC process, it suffers from the drawback of having a very large number of PDFs in the set; also, for many applications the non-Hessian framework may be a further drawback. However, the most essential features of the PDF uncertainties can be captured using three techniques that significantly reduce the number of error PDFs needed, especially in view of the fact that there is an uncertainty in the determination of the PDF uncertainties (witness the differences between the PDF groups at low x and high x), and therefore very high precision is not justified in view of the limited accuracy.

Two of these techniques use the Hessian formalism, considering only symmetric PDF uncertainties, while the third technique uses a compressed Monte Carlo technique, which allows for asymmetric uncertainties. Details of the derivations are provided in the PDF4LHC document. Correspondingly, three delivery options are available for the combined sets:

- `PDF4LHC15_mc`: contains 100 PDFs, including non-Gaussian features, constructed using the CMC method [50].
- `PDF4LHC15_30`: contains 30 PDFs in a Hessian framework, determined using the META-PDF technique [48].
- `PDF4LHC15_100`: contains 100 PDFs in a Hessian framework, determined using the MC2H approach [49].

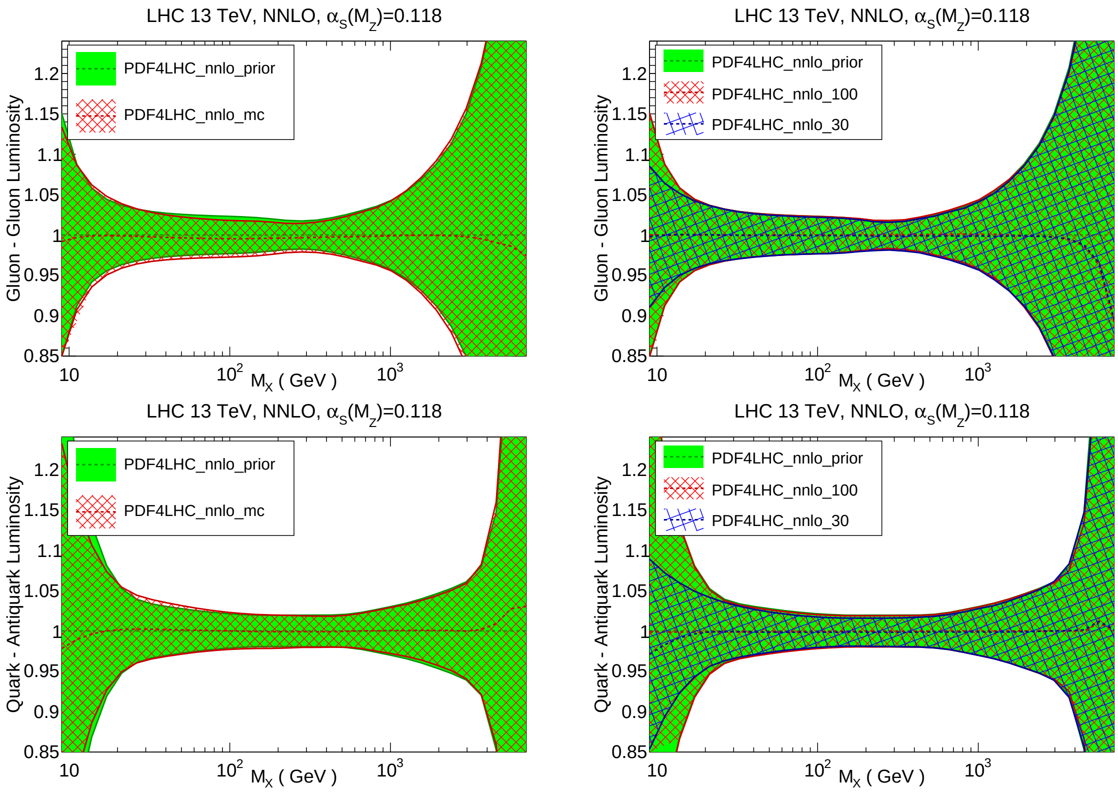

Figure 4: Comparison of parton luminosities at the LHC 13 TeV computed using the prior set `PDF4LHC15_nnlo_prior` with its compressed Monte Carlo representation, `PDF4LHC15_nnlo_mc` (left plots) and with its two Hessian sets, `PDF4LHC15_nnlo_100` and `PDF4LHC15_nnlo_30`. We show the gg (upper plots) and $q\bar{q}$ (lower plots) luminosities as a function of the invariant mass of the final state M_X, normalized to the central value of `PDF4LHC15_nnlo_prior`.

We will henceforth refer to the starting 900 replica Monte Carlo set as the “prior”, from which these reduced sets are constructed: `PDF4LHC15_nnlo_prior`.

A central value of $\alpha_s(m_Z) = 0.118$ is used for each of these sets, at both NLO and NNLO, with an uncertainty of $\delta\alpha_s(m_Z) = 0.0015$ as recommended in the chapter on Standard Model parameters of this document. Therefore, for each option, individual error sets using $\alpha_s(m_Z) = 0.1165$ and 0.1195 are provided in order to be able to compute the uncertainty due to $\delta\alpha_s(m_Z)$ in LHC cross-sections, which should be added in quadrature with the PDF uncertainty [35]. It has been verified that addition in quadrature is a good enough approximation (in some cases exact) to the exact recipes for PDF and α_s combination provided by each group [51–53].

The gluon-gluon and quark-antiquark PDF luminosities as a function of the final-state invariant mass M_X at the LHC 13 TeV are shown in Figure 4, where we compare the prior set `PDF4LHC15_nnlo_prior` with its compressed Monte Carlo representation, `PDF4LHC15_nnlo_mc` and with the two Hessian reduced sets, `PDF4LHC15_nnlo_100` and `PDF4LHC15_nnlo_30`. Note that by construction the central values of the two Hessian reduced sets coincide with the central value of the prior, while the central value of the Monte Carlo set reproduces it within the precision of the compression (which is seen to be quite high). All reduced sets correctly reproduce the uncertainty band for the 900 PDF Monte Carlo prior in the precision mass region and as the high mass region, while the `PDF4LHC15_30` shows a certain loss in precision when reproducing uncertainties for the very low mass region.

The three techniques for delivering the PDF4LHC PDF uncertainties are attempts to match the uncertainty bands produced from the prior, and not the bands from the three PDF groups *per se*. The degree of success is a measure of the precision of the three techniques for this purpose. It is therefore important not to confuse the precision of reproducing the prior with accuracy. The accuracy of the prior is not exactly known, especially at high and low mass, and the quoted PDF uncertainty represents only the best estimate by the PDF4LHC group.

I.2.3 Higgs boson production cross-sections

In Figure 5 we show representative inclusive Higgs boson production cross-sections in the relevant production channels at LHC with $\sqrt{s} = 13$ TeV: gluon-fusion, vector-boson fusion, associated production with a W boson, and associated production with a $t\bar{t}$ pair. These calculations have been performed with NLO matrix elements and NNLO PDFs, using `MG5_aMC@NLO` [54] interfaced to `aMCfast` [55] and `applgrid` [56], with the purpose of illustrating PDF uncertainties and also the relative difference between PDF sets. Indeed, since the NNLO/NLO K-factor is to a good approximation independent of PDFs, it should not affect the relative differences between the predictions of individual PDF sets. In this study, the Higgs bosons are left undecayed. No generation cuts are applied to Higgs bosons, jets or top quarks. The only selection cut that is applied is given by the fact that we assume that W and Z bosons decay leptonically, so the corresponding branching fraction is included and we require $p_T^l \geq 10$ GeV and $|\eta_l| \leq 2.5$ for the charged leptons from the weak boson decays. All uncertainties shown are pure PDF uncertainties, not including the uncertainty due to the value of α_s, which is fixed at $\alpha_s(m_Z) = 0.118$ for all cross-sections shown in the plot.

In each case, the predictions of the combined PDF4LHC15 prior and its three reduced versions, all normalized to the central value of the prior set, are shown along with the predictions from the sets which enter the combination, MMHT14, CT14 and NNPDF3.0. Predictions from the older global sets, MSTW08, CT10 and NNPDF2.3, which entered the previous prescription [28] are also shown for comparison. In particular, the better agreement for gluon-gluon fusion prediction using the new generation of PDFs (CT14, MMHT2014 and NNPDF3.0) compared to the older generation (CT10, MSTW08 and NNPDF2.3) is evident. In all cases, predictions using the reduced sets are in excellent agreement with those obtained using the prior.

In Figure 6 we show representative differential distributions for the Higgs boson production in gluon fusion, in particular the transverse momentum and rapidity distributions, at the LHC $\sqrt{s} = 13$ TeV, obtained using the three different deliveries of the combined set. The upper plots show the cross-section per bin, in pico-barns, while the lower plots show the corresponding results normalized to the central value of the PDF4LHC15 NNLO prior set. The three techniques agree well for these kinematic distributions, with a small offset for the predictions of the `PDF4LHC15_mc` set. Note that the transverse momentum distribution shown is a fixed-order result, and thus it is unreliable for $p_t \lesssim 30$ GeV where transverse momentum resummation effects become important.

I.2.4 Strong coupling and heavy quark masses

In order to estimate the further uncertainty due to the choice of α_s value it is useful to plot the cross-sections as a function of the value of $\alpha_s(m_Z)$. This is done in Figure 7, where the total inclusive cross-sections for Higgs boson production at $\sqrt{s} = 13$ TeV in different production channels are shown as a function of α_s for the three sets which enter the combination. In these plots we also include flavour predictions obtained using the ABM12 [40], HERAPDF2.0 [32] and JR14 [42] PDF sets, each at its preferred value of $\alpha_s(m_Z)$. In the case of ABM12, we use the $N_f = 5$ set. For HERAPDF2.0, we consider only the experimental PDF uncertainties. In the case of the JR14 set, we use the version determined in the variable-flavour-number scheme. Note that MMHT14, CT14, NNPDF3.0 and HERAPDF2.0 all use the same central value of the strong coupling, $\alpha_s(m_Z) = 0.118$; in the plot the values corresponding to these sets are slightly offset to improve readability. It is apparent from the figures which PDF sets can produce predictions that may fall substantially outside of the uncertainties of the three PDF sets that

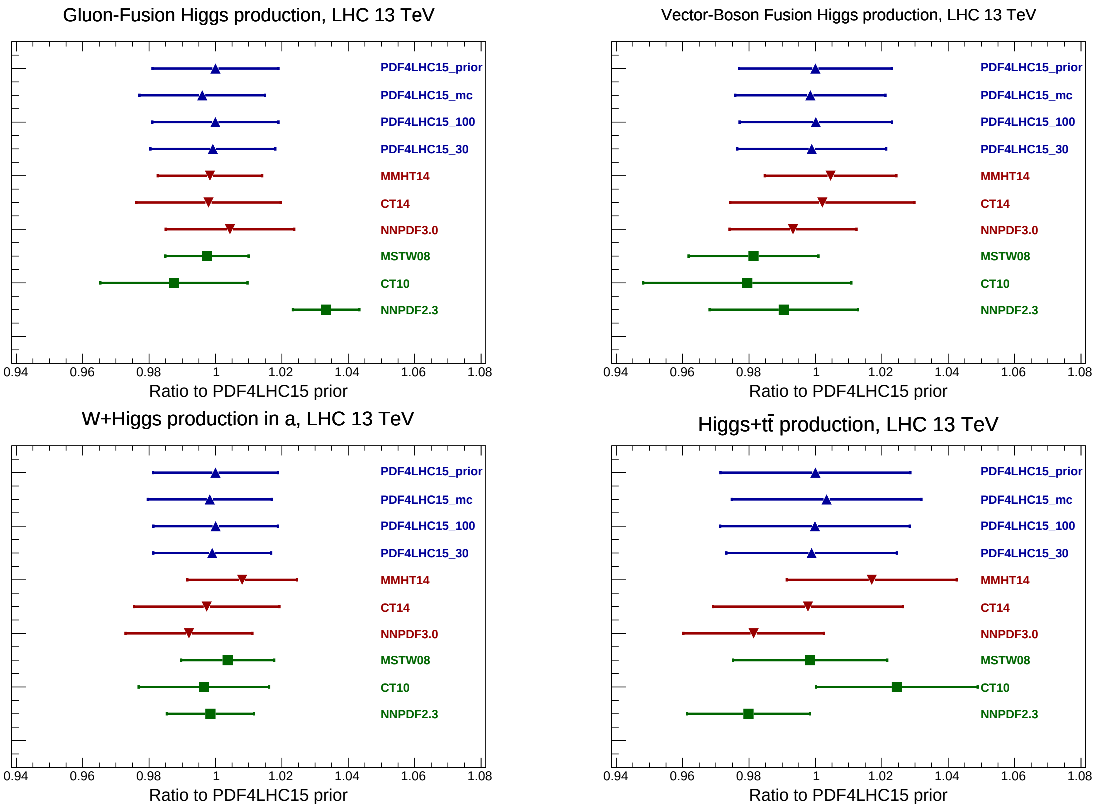

Figure 5: Inclusive Higgs boson production cross-sections at 13 TeV in the gluon-fusion, vector-boson fusion, associated production with W and associated production with a $t\bar{t}$ pair channels. In each case predictions of the three individual sets are shown along with those of the PDF4LHC15 prior and the three reduced sets, normalizing to the central value of the PDF4LHC15 prior set. Predictions obtained using the three older global sets which entered the previous PDF4LHC recommendation are also show. All cross-sections are computed at NLO with NNLO PDFs. The value of the strong coupling is fixed at $\alpha_s(m_Z) = 0.118$; the uncertainties shown are PDF uncertainties (not including the uncertainty due to $\alpha_s(m_Z)$).

enter the 2015 combination.

Unlike the case for the strong coupling $\alpha_s(M_Z)$, the different PDF groups do not use common values of the charm and bottom masses, and also use different definitions of a general mass variable number scheme (GM-VFN). These are two distinct issues, particularly since each group chooses the quark masses at fixed default values, as opposed to trying to determine them from a best fit, and the values chosen have no relation to the scheme choice.

Let us consider the issue of scheme choices first. Dependence on these has been very thoroughly studied in numerous articles [33, 57–60]. At NLO the variation in LHC cross section predictions for W and Z production due to quite extreme differences in choices of GM-VFN schemes can be of order $2-3\%$; they may be somewhat larger but still moderate especially at high scale for processes which are directly sensitive to charm, such as $Z+c$ or open charm production. However, as with other scheme choices in QCD, the ambiguity at fixed order is always an effect beyond the order of the calculation, and hence diminishes as one goes to higher orders. At NNLO scheme choices lead to changes in LHC cross section predictions of generally no more than 1%, and very often less. This can be appreciated from Figs. 11.6, 11.7 and 11.8 in [33], where differences between groups for the total HERA cross sections calculated using the same PDFs but different schemes can be at most $> 5\%$ at NLO, but never more than $1-2\%$ at NNLO. Differences in $F_2^{\bar{c}c}(x, Q^2)$, an observable which is directly sensitive to charm, which is much less precisely and widely measured at HERA, can be 30% in extreme cases at NLO but are rarely

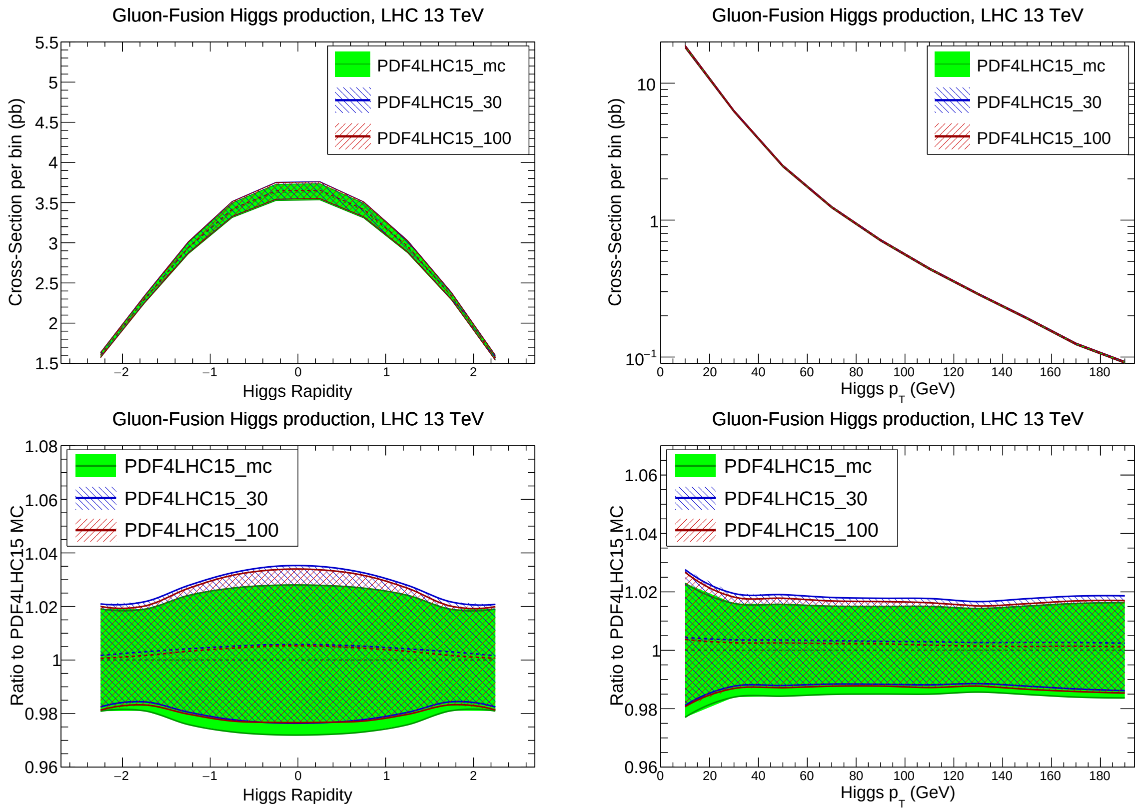

Figure 6: Differential distributions for Higgs boson production at gluon fusion at $\sqrt{s} = 13$ TeV. The Higgs boson rapidity (left) and transverse momentum (right) distributions are shown, using the three different deliveries of the combined PDF4LHC15 set. The upper plots show the absolute distributions, while in the lower plot results are normalized to the central value of the `PDF4LHC15_mc` set. Cross-sections have been computed at NLO with NNLO PDFs.

more than 10% at NNLO, and over most of the x, Q^2 range are much less than 5%. Hence, the variation due to the choice of GM-VFN scheme at NNLO is much less than the PDF uncertainty, and the variation between groups due to this can be taken as indicative of part on the theoretical uncertainty at NNLO. The variation due to adopting a FFN scheme would instead be quite large, and outside the PDF uncertainty.

The different PDFs used in the recommendation are all obtained using the heavy quarks defined in the pole mass scheme. However, the values chosen are different, with m_c ranging from 1.275–1.4 GeV and m_b from 4.18–4.75 GeV. The precise determinations of quark masses are performed in the $\overline{\text{MS}}$ scheme, and the conversion to the pole masses is imprecise due to a renormalon ambiguity in the conversion factor. In particular, the series for the charm quark shows essentially no convergence. Using the better behaved expression for the beauty mass, and the fact that $m_b^{\text{pole}} - m_c^{\text{pole}} = 3.4$ GeV with a very small uncertainty [27, 61], it was argued in [62] that a reasonable estimate for pole masses is $m_c^{\text{pole}} = 1.5 \pm 0.2$ GeV and $m_b^{\text{pole}} = 4.9 \pm 0.2$ GeV. Hence, the charm mass values chosen are perhaps slightly low, but not anomalous. The smallest m_b^{pole} value among the three combined sets is somewhat low, but the beauty data (including the contribution to total HERA cross sections) has extremely little constraint on PDFs in the global fit. Moreover, it has been argued that at lower orders a general mass variable flavour number scheme is not very sensitive to the scheme in which the mass is defined [63, 64]. The variation in the quark masses between groups, i.e. the deviations from the mean values, is relatively small compared to the intrinsic uncertainty for m_c, but a bit larger for m_b. As shown in [60, 64, 65], the Higgs cross section via gg fusion can vary by about 1% for m_c changes of about 0.2 GeV, while variations with m_b are much smaller than this, even for changes of 0.5 GeV. Hence, the variation in predictions

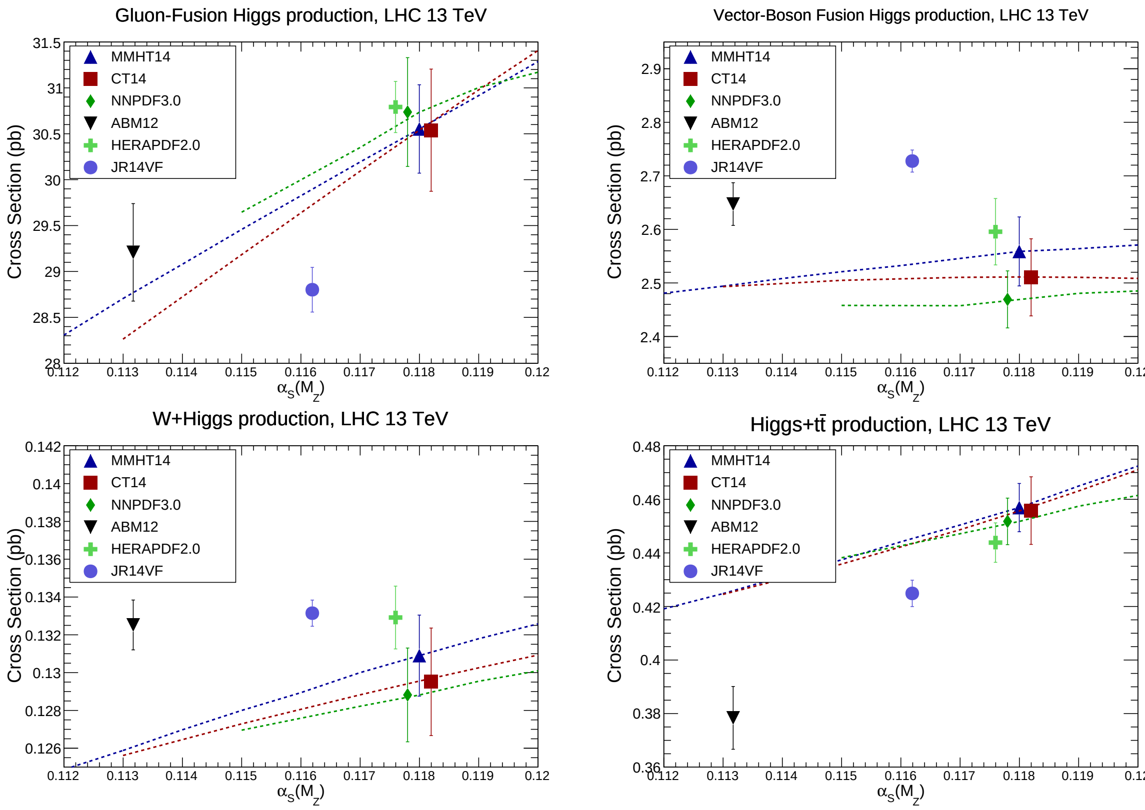

Figure 7: Dependence of the total inclusive cross-sections for Higgs boson production at $\sqrt{s} = 13$ TeV in different production channel on the value of the strong coupling $\alpha_s(m_Z)$ for the PDF sets which enter the combination: MMHT14, CT14, NNPDF3.0. Predictions obtained using ABM12, HERAPDF2.0, JR14VF NNLO sets are also shown at their preferred $\alpha_s(m_Z)$ value. The points shown for MMHT14, CT14, NNPDF3.0 and HERAPDF2.0 all refer to $\alpha_s(m_Z) = 0.118$ and are offset for clarity.

between the groups due to the different quark masses is generally much less than the PDF uncertainty, with the exception of cross sections directly dependent on the b quark distribution, where the mass effect on the distribution is more significant. The uncertainty due to quark masses should ideally be taken into account, and the current variation between groups should achieve this to some extent. However, in the future, it is probably preferable to settle on common mass values, perhaps defined in the $\overline{\text{MS}}$ scheme as advocated in [66], and a common uncertainty, as now done for $\alpha_s(M_Z)$.

For LHC calculations that are done in the $\overline{MS}$ scheme with up to 4 active quark flavours in the running α_s and PDFs, three combined PDF4LHC sets determined in this scheme are also provided. The respective PDF4LHC sets are constructed from 900 MC replicas of CT14, MMHT14, and NNPDF3.0 PDFs for $N_f = 4$ using the same combination techniques as for $N_f = 5$. In this case, the initial PDF parameterizations from the $N_f = 5$ fits at initial $Q_0 \sim m_c$ are evolved to higher Q including the lightest 4 flavours only. Contributions from massive bottom and top quarks should be then included in hard matrix elements. The input value $\alpha_s(M_Z, N_f = 4)$ in the $N_f = 4$ scheme is obtained from $\alpha_s(M_Z, N_f = 5) = 0.118$ by applying scheme transformation relations [67] at two or three loops in QCD, and assuming the average $m_b = 4.56$ GeV of the input PDF sets; it is thus rather smaller than the default value 0.118.

Table 1: Correlation coefficient between various Higgs boson production cross-sections and background cross-sections. In each case, the PDF4LHC15 NNLO prior set is compared to the Monte Carlo and with the two Hessian reduced sets. We also show the results from the three individual sets, CT14, MMHT14 and NNPDF3.0.

PDF Set	correlation coefficient					
	$t\bar{t}, Ht\bar{t}$	$t\bar{t}, hW$	$t\bar{t}, hZ$	$ggh, ht\bar{t}$	ggh, hW	ggh, hZ
PDF4LHC15_nnlo_prior	0.87	-0.23	-0.34	-0.13	-0.01	-0.17
PDF4LHC15_nnlo_mc	0.87	-0.27	-0.35	-0.10	0.07	-0.01
PDF4LHC15_nnlo_100	0.87	-0.24	-0.34	-0.13	-0.02	-0.17
PDF4LHC15_nnlo_30	0.87	-0.27	-0.43	-0.13	-0.04	-0.23
CT14	0.09	-0.32	-0.44	-0.26	-0.03	-0.18
MMHT14	0.90	-0.22	-0.52	0.08	-0.18	-0.33
NNPDF3.0	0.90	-0.17	-0.21	0.18	0.52	0.49

PDF Set	correlation coefficient					
	Z, W	$Z, t\bar{t}$	Z, ggh	$Z, ht\bar{t}$	Z, hW	Z, hZ
PDF4LHC15_nnlo_prior	0.89	-0.49	0.08	-0.46	0.56	0.74
PDF4LHC15_nnlo_mc	0.90	-0.44	0.18	-0.42	0.62	0.80
PDF4LHC15_nnlo_100	0.91	-0.48	0.09	-0.46	0.59	0.74
PDF4LHC15_nnlo_30	0.88	-0.63	0.04	-0.61	0.56	0.72
CT14	0.92	-0.69	0.12	-0.69	0.69	0.77
MMHT14	0.76	-0.70	0.12	-0.83	0.15	0.43
NNPDF3.0	0.96	-0.13	0.62	-0.30	0.84	0.85

PDF Set	correlation coefficient					
	$W, t\bar{t}$	W, ggh	$W, ht\bar{t}$	W, hW	W, hZ	$t\bar{t}, ggh$
PDF4LHC15_nnlo_prior	-0.40	0.20	-0.40	0.76	0.77	0.30
PDF4LHC15_nnlo_mc	-0.44	0.26	-0.42	0.81	0.82	0.32
PDF4LHC15_nnlo_100	-0.40	0.20	-0.40	0.76	0.77	0.30
PDF4LHC15_nnlo_30	-0.47	0.19	-0.47	0.77	0.76	0.31
CT14	-0.56	0.22	-0.56	0.80	0.77	0.09
MMHT14	-0.47	0.24	-0.53	0.62	0.63	0.46
NNPDF3.0	-0.08	0.64	-0.26	0.88	0.86	0.51

I.2.5 PDF correlations

Also of importance for Higgs boson predictions and analyses are the PDF correlations, both among Higgs boson production processes and between Higgs boson processes and potential background processes: tables of correlations obtained using various PDF sets were given in the previous Yellow Report [9]. These tables can now be updated using the more recent combined set. In Table 1 we collect the correlation coefficients between different Higgs boson production channels, as well as between representative Higgs boson signal and background processes. We show the results for the PDF4LHC15 NNLO prior and for the three reduced combined PDF sets, and we also include the results for the three individual PDF sets. The cross-sections have been computed at NLO with NNLO PDFs, using the same settings as in previous plots. All of the techniques do reasonably well reproducing the correlations of the prior, with the PDF4LHC15_100 PDFs reproducing the prior to within a per cent.

It should be emphasized that the values of the correlation themselves, however, can be viewed as only having a single digit (or less) accuracy in the sense that the PDF correlations for Higgs processes and backgrounds for the 3 global PDF sets can differ by the order of 0.2 (or more). For example, the spread in correlation coefficients for gluon-gluon fusion production and associated (Zh) production is 0.67. Note that the differences in the correlation coefficients between NNPDF3.0, CT14 and MMHT14 are large in many cases, though there is also good agreement in other cases.

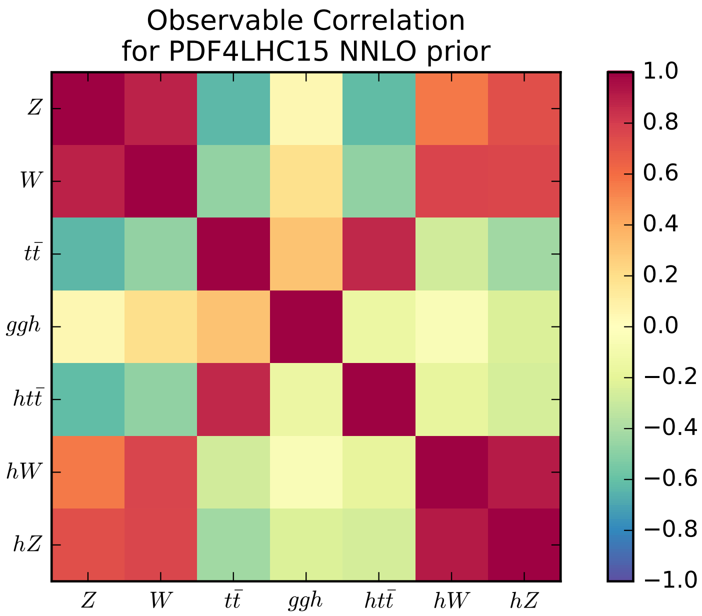

Figure 8: The value of the correlation coefficient between representative Higgs boson signal and background processes at the LHC 13 TeV, using the PDF4LHC15NNLO prior. The colour of each entry of the correlation matrix indicates the absolute size of the correlation coefficient. The processes shown in this figure are ggh, $ht\bar{t}$, hW and hZ (for signal) and Z, W and $t\bar{t}$ (for backgrounds).

In Figure 8 we show the absolute value of the correlation coefficient between representative Higgs boson signal and background processes at the LHC 13 TeV, using the PDF4LHC15NNLO prior. The colour of each entry of the correlation matrix indicates the absolute size of the correlation coefficient, with a granularity of 0.2. The processes shown in this figure are ggh, $ht\bar{t}$, hW and hZ (for signal) and Z, W and $t\bar{t}$ (for backgrounds). Very similar results are obtained if any of the three reduced sets is used.

I.2.6 Acceptance calculations

An important application of the PDF4LHC15 combined sets is the calculation of PDF uncertainties in acceptances. These are defined as the ratio of cross-sections with fiducial selection cuts to the corresponding inclusive cross-section, $\mathcal{A} = (\sigma|_{\rm fid})/(\sigma|_{\rm incl})$. To illustrate this usage, we have computed the acceptances, with the corresponding PDF uncertainties, for two Higgs boson production processes with experimentally realistic selection cuts, namely:

- Higgs boson production in the gluon fusion process, decaying into diphotons, $gg \to h \to \gamma\gamma$,
- Higgs boson production in association with a W boson, with the latter decaying leptonically, $pp \to hW^{\pm} \to hl^{\pm}\nu_l$.

As in the rest of this chapter, the calculations have been performed for the LHC 13 TeV with `MG5_aMC@NLO` interfaced to `aMCfast`, using NNLO PDFs with NLO matrix elements.

In the calculation of the fiducial cross-sections, we use similar acceptance requirements as those in the corresponding ATLAS and CMS analyses. For both processes, jets are reconstructed with the anti-k_T algorithm with $R = 0.4$, and they satisfy $p_T \geq 30$ GeV and $|\eta| \leq 4.4$. The additional selection cuts in the case of the $gg \to h \to \gamma\gamma$ are the following: for photons we require $p_T \geq 25$ GeV and $\eta \leq 2.4$, and the invariant mass of the diphotons should satisfy $|m_{\gamma\gamma} - 125\ \text{GeV}| \leq 15$ GeV. In the case of Higgs associated production, $pp \to hW^{\pm} \to hl^{\pm}\nu_l$, the selection cuts on the charged leptons are $|\eta_l| \leq 2.5$ and $p_T^l \geq 20$ GeV.

Using these kinematical cuts, we have generated applgrids for both fiducial and inclusive cross-sections, and computed the resulting acceptance corrections and the corresponding PDF uncertainties. In Table 2 we collect the value of the acceptances $\mathcal{A}$ in each case, together with the corresponding PDF uncertainties computed with the PDF4LHC15 prior and with the three reduced sets. For completeness, we also show the results for the acceptances computed with the individual PDF sets. We observe excellent agreement between the acceptances computed with the prior and with the three reduced sets, both for the central value and for the PDF uncertainties.

Table 2: The acceptance corrections $\mathcal{A}$ for Higgs boson production at the LHC 13 TeV in two different channels with realistic selection cuts, and the corresponding PDF uncertainties. We compare the results of the PDF4LHC15 NNLO prior with the three reduced sets. For completeness, we also show the results for the acceptances computed with the individual PDF sets. See text for more details of the specific selection cuts in each case.

	$\mathcal{A}(gg \to h \to \gamma\gamma)$	$\mathcal{A}(pp \to hW \to hl\nu_l)$
PDF4LHC15 prior	0.728 +- 0.006 (0.9%)	0.7536 +- 0.0014 (0.18%)
PDF4LHC15_mc	0.727 +- 0.006 (0.9%)	0.7538 +- 0.0015 (0.20%)
PDF4LHC15_100	0.728 +- 0.006 (0.9%)	0.7536 +- 0.0013 (0.17%)
PDF4LHC15_30	0.728 +- 0.006 (0.9%)	0.7536 +- 0.0012 (0.15%)
MMHT14	0.728 +- 0.004 (0.6%)	0.7532 +- 0.0012 (0.15%)
CT14	0.725 +- 0.007 (1.0%)	0.7543 +- 0.0014 (0.18%)
NNPDF3.0	0.730 +- 0.005 (0.7%)	0.7534 +- 0.0011 (0.14%)

I.2.7 Summary

To summarize, in Table 3 we collect the available PDF4LHC15 NNLO $N_f = 5$ combined sets. The corresponding sets are also available at NLO, as well as $N_f = 4$ versions. All the combined PDF4LHC14 sets are available through LHAPDF6 [43], which also includes built-in routines for the calculation of the PDF and PDF+α_s uncertainties for all relevant cases.

Recommendations for the usage of each of these techniques are given in the PDF4LHC 2015 document [35], along with explicit formulae for the calculation of PDF and PDF+$\alpha_s(m_Z)$ uncertainties for each of the techniques. The recommendations can be simply summed up. If asymmetric uncertainties are important, for example at high mass, and Hessian errors are not essential, then PDF4LHC15_mc should be used. There are two options for Hessian uncertainties. The PDF4LHC15_30 set provides a good estimate of the uncertainty of the prior with fewer members, sufficient in many cases, such as for the determination of nuisance parameters or acceptance calculations. To reproduce the uncertainty of the prior exactly, then the PDF4LHC_100 sets should be used.

Table 3: Summary of the combined NNLO PDF4LHC15 sets with $N_f^{\max} = 5$ that are available from `LHAPDF6`. The corresponding NLO sets are also available. Members 0 and 1 of `PDF4LHC15_nnlo_asvar` coincide with members 101 and 102 (31 and 32) of `PDF4LHC15_nnlo_mc_pdfas` and `PDF4LHC15_nnlo_100_pdfas` (`PDF4LHC15_nnlo_30_pdfas`). Recall that in `LHAPDF6` there is always a zeroth member, so that the total number of PDF members in a given set is always $N_{\rm mem} + 1$. See text for more details.

`LHAPDF6` grid	Pert order	`ErrorType`	$N_{\rm mem}$	$\alpha_s(m_Z^2)$
`PDF4LHC15_nnlo_mc`	NNLO	`replicas`	100	0.118
`PDF4LHC15_nnlo_100`	NNLO	`symmhessian`	100	0.118
`PDF4LHC15_nnlo_30`	NNLO	`symmhessian`	30	0.118
`PDF4LHC15_nnlo_mc_pdfas`	NNLO	`replicas+as`	102	mem 0:100 $\to$ 0.118
				mem 101 $\to$ 0.1165
				mem 102 $\to$ 0.1195
`PDF4LHC15_nnlo_100_pdfas`	NNLO	`symmhessian+as`	102	mem 0:100 $\to$ 0.118
				mem 101 $\to$ 0.1165
				mem 102 $\to$ 0.1195
`PDF4LHC15_nnlo_30_pdfas`	NNLO	`symmhessian+as`	32	mem 0:30 $\to$ 0.118
				mem 31 $\to$ 0.1165
				mem 32 $\to$ 0.1195
`PDF4LHC15_nnlo_asvar`	NNLO	-	1	mem 0 $\to$ 0.1165
				mem 1 $\to$ 0.1195